

Assessment of the Potential Advantages of Distributed-Propulsion for Aircraft

Andy Ko*, J.A. Schetz[†] and William H. Mason[‡]

*Multidisciplinary Analysis and Design Center for Advanced Vehicles
Virginia Polytechnic Institute and State University
Blacksburg, VA 24061-0203*

The basic idea behind the distributed-propulsion concept considered here is to duct part of the aircraft engine exhaust to exit out along the trailing edge across part or all of the span of the wing. There has been a conjecture that there will be an increase in propulsive efficiency when there is blowing out of the trailing edge of the wing. A mathematical formulation was derived to explain this. The formulation showed that the jet ‘fills in’ the wake behind the body, improving the overall aerodynamic/propulsion system, resulting in an increased propulsive efficiency. A model to represent this phenomenon was also derived for implementation into a Multidisciplinary Optimization (MDO) framework. Together with other models of distributed-propulsion effects, this influence was integrated into a Blended-Wing-Body (BWB) MDO design program. A distributed-propulsion BWB aircraft design was optimized for minimum takeoff gross weight and compared to a similarly designed conventional BWB aircraft. The distributed-propulsion BWB aircraft was found to be 4.4% lighter than the conventional BWB design, and it used 2.7% less fuel. Other potential benefits of distributed-propulsion are the elimination of control surfaces and a reduction of perceived noise.

1. Introduction

One suggested distributed-propulsion arrangement on an aircraft is for an array of small engines distributed along the wings and/or around the fuselage under cowls as depicted schematically in Figure 1. Such an arrangement is unlikely to be a feasible and beneficial design concept. The main reason is the basic conflict between the axisymmetric geometry of jet or propeller engines and the planar space under a cowl. If the engines are turbojets, little additional air will be entrained to flow under the cowl resulting in poor system propulsive efficiency. If the engines are turbofans, the flow in the irregular spaces under the cowl and surrounding the fans will have high drag and will not contribute to propulsion. Thus, we have rejected further consideration of this kind of distributed-propulsion arrangement. Rather, we have selected a concept that ducts part of the exhaust from a modest number of wing mounted engines out of the trailing edge across part or all of the span of the wing. Such a concept could be employed as a seamless high-lift system, dispensing with conventional high-lift systems that are major sources of noise. Figure 2 shows the wing spanwise cuts illustrating this concept.

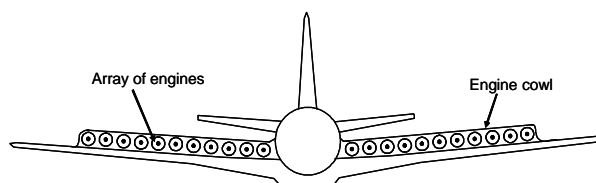


Figure 1: Front view schematic of a distributed-propulsion configuration.

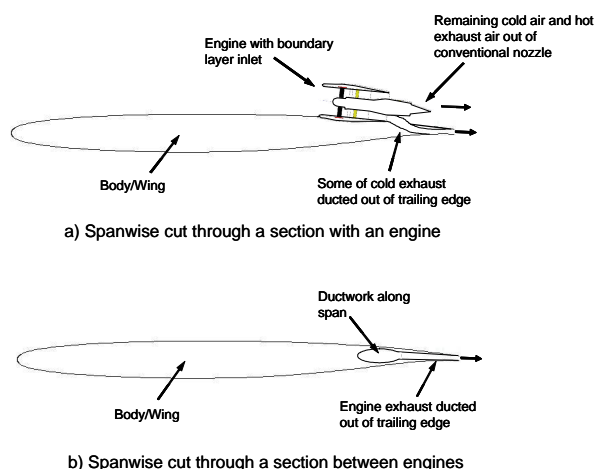


Figure 2: Drawing of wing spanwise cross sections through a location with an engine and a location between engines of the distributed-propulsion concept wing.

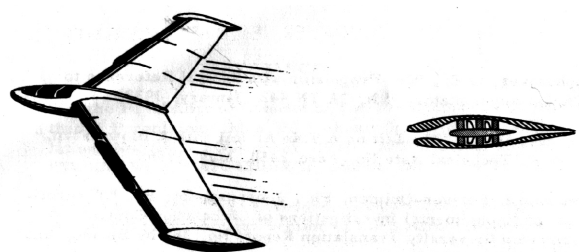
*Graduate research assistant. Member AIAA.

[†]Fred D. Durham Endowed Chair, Fellow AIAA.

[‡]Professor, Associate Fellow AIAA.

Copyright © 2003 by Andy Ko, Joseph A. Schetz and William H. Mason. Published by the American Institute of Aeronautics and Astronautics, Inc., with permission.

A major potential aerodynamic benefit of this distributed-propulsion arrangement is the synergistic integration between the propulsion system and aircraft airframe. The idea of an integrated propulsion/lift system is already evident in nature, where animals in flight generate lift and thrust using the same organs. Kuchemann[§] [1], proposed a ‘jet wing’ configuration to improve propulsive efficiency. A jet wing configuration incorporates the propulsion system by burying the engine in the wing and letting the engine exhaust out the trailing edge as shown in Figure 3. Kuchemann [2] suggests that this jet wing arrangement may be more efficient than a conventional engine arrangement where the engine nacelles are installed somewhere away from the wings and body. This paper will consider Kuchemann’s assertion that this arrangement improves the propulsive efficiency.



KUCHEMANN'S
JET WING AIRCRAFT

SCHEMATIC
OF JET WING

Figure 3: Kuchemann’s Jet Wing Aircraft concept [1].

The idea of distributed-propulsion for aircraft has been suggested with the objective of reducing noise [3]. Distributing the propulsion system using a number of small engines instead of a few large ones could reduce the total propulsion system noise. There are other potential benefits of distributed-propulsion. One advantage is its improved safety due to engine redundancy. With numerous engines, an engine-out condition is not as critical to the aircraft’s performance in terms of loss of available thrust and controllability. The load redistribution provided by the engines has the potential to alleviate gust load/flutter problems, while providing passive load alleviation resulting in a lower wing weight. There is also the possible improvement in affordability due to the use of smaller, easily-interchangeable engines.

[§] The original reference to Kuchemann introducing the jet wing concept has been cited to be in: “On the Possibility of Connecting the Production of Lift with that of Propulsion,” *M.A.P. Volkenrode, Reports and Translations* No. 941 – 1 Nov., 1947, APPENDIX I, Kuchemann, D., “The Jet Wing.” However, we were unable to obtain a copy of this reference.

2. Distributed-propulsion and propulsive efficiency

When Kuchemann introduced the jet wing concept in 1938 [1], he suggested that this configuration would result in an improvement in propulsive efficiency. Although this conjecture is plausible in theory, no detailed assessment has been found in the literature. The improvement in propulsive efficiency comes from the general idea that the jet exiting the trailing edge of the wing ‘fills in the wake’ behind the wing. This approach is commonly implemented in ships and submarines, having a streamlined axisymmetric body (neglecting the sail and the control surfaces) and a single propeller on the axis. Although the wake is not perfectly filled, this arrangement tends to maximize the propulsive efficiency of the entire system [4]. It is expected that a similar improvement in propulsive efficiency can be achieved with a proposed distributed-propulsion configuration that ducts some of the engine exhaust out of the trailing edge of the aircraft.

The Froude Propulsion Efficiency, h_p , can be defined as the ratio of useful power out of the propulsor to the rate of kinetic energy added to the flow by the propulsor, as shown in Equation (2.1) [5].

$$h_p = \frac{T U_\infty}{q S_{ref} U_\infty \mathbf{b} (\mathbf{b}^2 - 1)} \quad (2.1)$$

where T = Thrust

U_∞ = Freestream velocity

S_{ref} = Reference area

q = dynamic pressure

\mathbf{b} = ratio of the engine jet velocity to the freestream velocity

For simplicity, consider initially a two-dimensional, non-lifting, self-propelled vehicle with an engine as shown in Figure 4. The wake of the body is taken as independent of the jet from the engine. For the system to be self-propelled, the drag associated with the

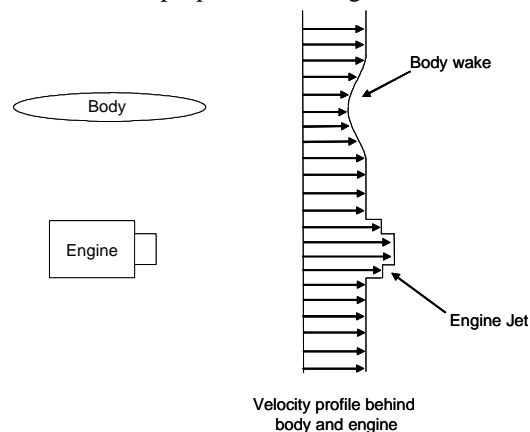


Figure 4: A typical velocity profile behind a body and engine

velocity deficit due to the wake is balanced by the thrust of the engine. The loss in propulsive efficiency is due to any net kinetic energy left in the wake (characterized by the non-uniformities in the velocity profiles) compared to that of a uniform velocity profile. For this case, a typical Froude Propulsion Efficiency for a high bypass ratio turbofan at Mach 0.85 is 80% [5].

Now, consider a distributed-propulsion configuration where the jet and the wake of the body are combined, as shown in Figure 5. In an ideal distributed-propulsion system, the jet will perfectly ‘fill in’ the wake creating a uniform velocity profile. The kinetic energy added to the flow by the propulsor compared to that of a uniform velocity profile is therefore zero, which results in a Froude Propulsive Efficiency of 100%. In practice, the jet does not fully ‘fill in’ the wake but produces smaller non-uniformities in the velocity profile as illustrated in Figure 6. However, this velocity profile will result in a smaller net kinetic energy than that of the case where the body and engine are independent shown in Figure 4. The efficiency associated with a distributed-propulsion configuration will be bounded by the efficiency of the decoupled body/engine case (nominally at 80%) and the perfect distributed-propulsion configuration of 100%. It should be noted, however, that we have not included the effect the jet has on the pressure distribution of the body. We expect that the jet will entrain the flow over the surface and increase the drag, but this effect is not modeled here.

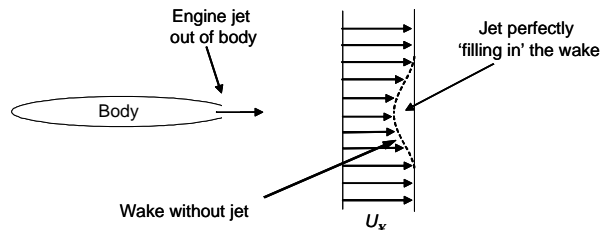


Figure 5: The velocity profile of a perfect distributed-propulsion body/engine system.

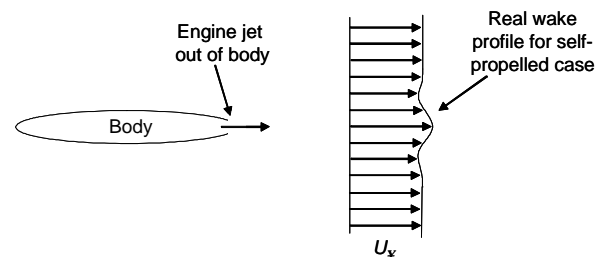


Figure 6: The velocity profile of a realistic distributed-propulsion body/engine system.

Now consider a lifting body with an engine in a distributed-propulsion configuration. In this case, the drag on the system is not only due to the viscous drag

but also the drag due to the downwash. This means that the engine jet now ‘overfills’ the wake. Therefore, even in a perfect system, a 100% Froude Propulsive Efficiency is not attainable. In the perfect system of this configuration, part of the jet would be used to perfectly ‘fill in’ the wake while the remaining jet would be in the freestream away from the body in order to overcome the induced drag. This arrangement is like that of our distributed propulsion concept illustrated in Figure 2. If the induced drag constitutes about 50% of the total drag (viscous drag + induced drag) as in well designed wings, then the maximum possible increase in Froude Propulsive Efficiency will be half of that in the non-lifting body case, i.e. the Froude Propulsive Efficiency using a nominal high bypass ratio turbofan in a distributed-propulsion setting would be between 80% -90%.

From the above example for a subsonic lifting body, we see that the upper limit of the Froude propulsive efficiency is determined by the ratio of the viscous drag to the total drag. In the same way, for a lifting body in transonic flow, the upper limit of the Froude propulsive efficiency is determined by the ratio of the viscous and wave drag to the total drag. The wave drag is included because the presence of shocks on the body affects the size and shape of the wake behind the wing/body.

In an aircraft design performance assessment, the Froude Propulsive Efficiency can be reflected in the performance in terms of the thrust specific fuel consumption (SFC). We should expect that an increase in the Froude Propulsive Efficiency will result in a reduction in SFC, improving the aircraft’s overall performance.

To relate the Froude Propulsive Efficiency to SFC, consider the approximate relation given in Equation (2.2) by Stinton [6].

$$SFC = \frac{U_\infty}{k_1 h_p h_t} \quad (2.2)$$

where U_∞ = freestream velocity

k_1 = SFC factor. Stinton [6] determined this factor to be 4000 ft-hr/s.

h_p = Froude propulsive efficiency

h_t = the engine internal thermal efficiency

Assuming a constant freestream velocity, SFC factor and internal engine thermal efficiency, we can obtain Equation (2.3).

$$\frac{sf_{c_1}}{sf_{c_2}} = \frac{h_{p_2}}{h_{p_1}} \quad (2.3)$$

Hence, given a baseline propulsive efficiency and SFC, a new SFC can be calculated for an increase in propulsive efficiency.

Now that the maximum and minimum limits in attainable propulsive efficiency have been determined, we would expect that only a percentage of this possible increase in propulsive efficiency can be achieved. In implementing this formulation into an MDO framework, we assumed that only 25% of the maximum possible savings in propulsive efficiency could be attained.

In this model development, we have assumed that the jet is able to fill in the wake, and that the efficiencies that are proposed can be achieved. However, we still have not given an analysis illustrating this effect. To do this, we now provide an analysis of an idealized model problem

3. Distributed-Propulsion Theory

Consider a two-dimensional body in a flow that is self-propelled by an engine whose jet does not influence the wake of the body. The thrust that is produced by the engine is described in Equation (3.1) [5].

$$T = \dot{m}_a [(1+f)U_j - U_\infty] + (p_e - p_\infty)A_e \quad (3.1)$$

where \dot{m}_a = airflow rate

f = fuel-air ratio

U_j = velocity out of the engine

p_e = exhaust pressure

p_∞ = ambient pressure

A_e = exhaust area

We will assume that the exhaust pressure is equal to the ambient pressure, and that the fuel mass flow compared to the air mass flow is negligible. The thrust equation therefore reduces to:

$$T = \dot{m}_a (U_j - U_\infty) \quad (3.2)$$

The kinetic energy added to the flow by the propulsor is given as:

$$\Delta KE = \frac{1}{2} \dot{m}_a [(1+f)U_j^2 - U_\infty^2] \quad (3.3)$$

approximated as:

$$\Delta KE = \frac{1}{2} \dot{m}_a (U_j^2 - U_\infty^2) \quad (3.4)$$

Using the definition of the Froude Propulsive Efficiency, Equation (3.2) and (3.4), we get:

$$\begin{aligned} h_p &= \frac{\dot{m}_a (U_j - U_\infty) U_\infty}{\frac{1}{2} \dot{m}_a (U_j^2 - U_\infty^2)} \\ &= \frac{2}{\frac{U_j}{U_\infty} + 1} \end{aligned} \quad (3.5)$$

The force vector, according to the momentum theorem and conservation of mass, is shown in Equation (3.6).

$$\mathbf{F} = -\iint_S (p - p_\infty) d\mathbf{S} - \iint_S \mathbf{r} \mathbf{q} (U_\infty + \mathbf{q}) dS \quad (3.6)$$

where \mathbf{F} = force vector

p = pressure at the boundaries

\mathbf{q} = velocity perturbation from U_∞ , comprised of components u, v, w

\mathbf{r} = density

S = Control surface

Consider a two-dimensional control volume around the body and the engine, as in Figure 7. For simplicity, assume that the wake of the body and jet of the engine take on square shapes. Again, assume that the downstream pressure is undisturbed from the upstream (or ambient) pressure. For the force in the freestream direction, Equation (3.6) reduces to:

$$F_x = -\int_{-h}^h \mathbf{r} u (U_\infty + u) dy \quad (3.7)$$

where u is the velocity perturbation from U_∞ in the freestream direction.

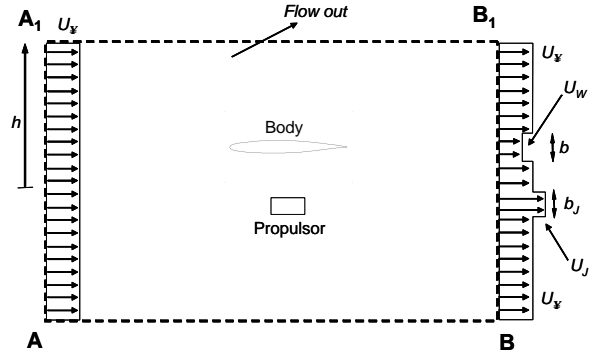


Figure 7: Control surface around the non-distributed-propulsion configuration where the body is independent of the propulsor

Performing the integration in for the profile in Figure 7, results in

$$F_x = \mathbf{r} [b_w U_w (U_\infty - U_w) - b_j U_j (U_j - U_\infty)] \quad (3.8)$$

Equating the force to zero for a self-propelled case, and rearranging, we obtain

$$\left(\frac{U_J}{U_\infty}\right)^2 - \left(\frac{U_J}{U_\infty}\right) - \left(\frac{b_J}{b_w}\right)^{-1} \left(\frac{U_w}{U_\infty}\right) \left(1 - \frac{U_w}{U_\infty}\right) = 0 \quad (3.9)$$

Solving for U_J/U_∞ , we get

$$\frac{U_J}{U_\infty} = \frac{1}{2} \pm \frac{1}{2} \sqrt{1 + 4 \left(\frac{b_J}{b_w}\right)^{-1} \left(\frac{U_w}{U_\infty}\right) \left(1 - \frac{U_w}{U_\infty}\right)} \quad (3.10)$$

Since $U_w/U_\infty \leq 1.0$, the term in the square root will have a value greater than 1.0. Since $U_J/U_\infty \geq 1.0$, the positive solution is applicable.

$$\frac{U_J}{U_\infty} = \frac{1}{2} + \frac{1}{2} \sqrt{1 + 4 \left(\frac{b_J}{b_w}\right)^{-1} \left(\frac{U_w}{U_\infty}\right) \left(1 - \frac{U_w}{U_\infty}\right)} \quad (3.11)$$

Substituting Equation (3.11) into Equation (3.5), the propulsive efficiency for the non-distributed-propulsion configuration is:

$$h_p = \frac{2}{\frac{3}{2} + \sqrt{1 + 4 \left(\frac{b_J}{b_w}\right)^{-1} \left(\frac{U_w}{U_\infty}\right) \left(1 - \frac{U_w}{U_\infty}\right)}} \quad (3.12)$$

We see that the propulsive efficiency is at 100%, if $U_J/U_\infty = 1.0$ (corresponding to $b_J/b_w = \infty$).

Now, consider the case where the jet of the engine is superimposed within the wake of the body, modeling the distributed-propulsion configuration as shown in Figure 8

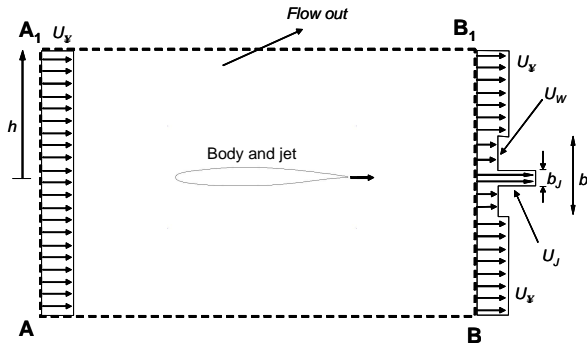


Figure 8: Control surface around the distributed-propulsion configuration where the jet from the propulsor is combined with the wake of the body.

Performing the integration in Equation (3.7) across the control surface for the profile in Figure 8, we get:

$$F_x = r \left[b_w (U_w^2 - U_\infty U_w) + b_J (U_J^2 - U_w^2 + U_\infty U_w - U_\infty U_J) \right] \quad (3.13)$$

Equating the force to zero for a self-propelled case, and rearranging, gives:

$$\frac{U_J}{U_\infty} = \frac{1}{2} \pm \frac{1}{2} \sqrt{1 + 4 \left(\frac{U_w}{U_\infty}\right) \left(1 - \frac{U_w}{U_\infty}\right) \left[\left(\frac{b_J}{b_w}\right)^{-1} - 1\right]} \quad (3.14)$$

Again, since $U_w/U_\infty \leq 1.0$, and $U_J/U_\infty \geq 1.0$, the positive solution is applicable, yielding:

$$\frac{U_J}{U_\infty} = \frac{1}{2} + \frac{1}{2} \sqrt{1 + 4 \left(\frac{U_w}{U_\infty}\right) \left(1 - \frac{U_w}{U_\infty}\right) \left[\left(\frac{b_J}{b_w}\right)^{-1} - 1\right]} \quad (3.15)$$

Substituting Equation (3.15) into Equation (3.5), we get the mathematical formulation for a distributed-propulsion case as:

$$h_p = \frac{2}{\frac{3}{2} + \frac{1}{2} \sqrt{1 + 4 \left[\left(\frac{b_J}{b_w}\right)^{-1} - 1\right] \left(\frac{U_w}{U_\infty}\right) \left(1 - \frac{U_w}{U_\infty}\right)}} \quad (3.16)$$

Now, consider the limiting case in this arrangement. For the propulsive efficiency to be 100%, it is required that $b_J/b_w = 1.0$. This corresponds to $U_J/U_\infty = 1.0$. In essence, it is the case where the jet ‘perfectly’ fills in the wake of the body. This effect is consistent with our previous assertion that a perfectly filled wake corresponds to an efficiency of 100%. It should be noted that the value of $b_J/b_w \leq 1.0$, and a consideration of b_J/b_w values larger than 1.0 would involve a new formulation. $U_J/U_\infty \geq 1.0$, as the system cannot be self-propelled for any value of $U_J/U_\infty < 1.0$.

Figure 9 shows a plot of the propulsive efficiency using Equations (3.12) and (3.16) for different values of b_J/b_w , at a specified representative value of $U_w/U_\infty = 0.5$. It clearly shows that the distributed-propulsion configuration achieves a higher propulsive efficiency than the non-distributed-propulsion configuration for the same value of b_J/b_w .

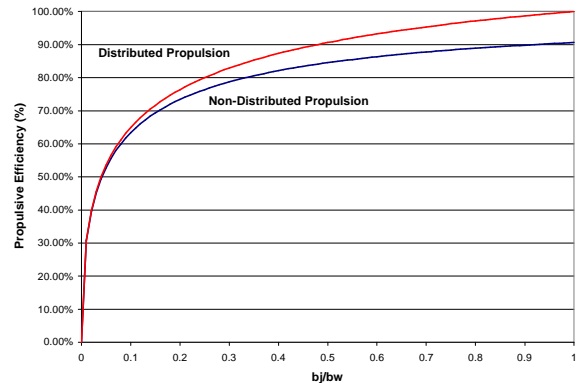


Figure 9: Froude propulsive efficiency versus b_J/b_w for distributed-propulsion and non-distributed-propulsion configurations. $U_w/U_\infty = 0.5$.

Although Figure 9 plots values of b_j/b_w of up to 1.0, b_j/b_w is not limited to this maximum value for the non-distributed-propulsion case. In fact, we find from Equation (3.12) that as b_j/b_w is increased towards infinity, the propulsive efficiency for the non-distributed-propulsion case tends towards 100%.

Before we discuss the implications of this formulation, it is prudent to address the validity of the assumptions that were made and their influence in the overall context of the subject. First, we assumed that the jet exit pressures are equal to the surrounding ambient pressure. This assumption is usually made to represent a propulsion system that is working at its optimum design configuration. One could repeat the above formulation taking into account the pressure terms, but this complicates the results, and does not provide any additional insight. Second, we assumed that the fuel mass flow rate compared to the air mass flow rate is negligible. This assumption is reasonable, and holds for most turbofan engines, especially for high bypass ratio turbofan engines. Next, we assumed a square-shaped velocity profile for the wake and the jet. The formulation was repeated assuming a triangular jet and wake velocity profiles [7]. The results show that the savings for a triangular shaped wake and jet is not as high as that for a square shaped wake and jet. For example, for $b_j/b_w = 0.4$ and $U_w/U_j = 0.5$, the difference in propulsive efficiencies between the distributed-propulsion case and the non-distributed-propulsion case by 1.75% using a triangular shaped jet and wake assumption versus 5.19% for a square shaped jet and wake assumption. By considering both the square and triangular shaped velocity profiles, we essentially were considering the limiting profile shapes for a wake and a jet. A realistic wake and jet will possess a shape in between that of the square and triangular shape. Implied in the formulation of the theory, we had assumed a linear superposition of the jet and wake when considering the distributed-propulsion configuration. Also, we assumed that the size of the wake remains the same as that in the non-distributed-propulsion configuration. In reality, there will undoubtedly be interaction effects such as entrainment of the flow by the jet, altering the flow field on the airfoil, which may increase the drag.

Let us apply this theory to a transonic passenger transport aircraft where we assume that supercritical airfoil sections will be used. One major characteristic of supercritical airfoils is the presence of a thick (or even diverging) trailing edge. The presence of this thick trailing edge significantly decreases the wave drag at transonic Mach numbers compared to a similar airfoil design with a closed trailing edge [8]. However, the presence of the thick trailing edge also results in the formation of a recirculation region immediately behind

the airfoil, resulting in a base drag penalty. At transonic Mach numbers, the reduction in wave drag is much greater than the base drag due to the thick trailing edge, resulting in a better overall airfoil L/D performance. The penalties of this base drag are considered an ‘expense’ at sub-critical Mach numbers in return for the drag performance at transonic Mach numbers [8]. A common trailing edge thickness for a supercritical airfoil is approximately 0.7% of the airfoil chord length. For example, a 20 ft chord length section will result in a 1.8 inch trailing edge thickness. Such a thickness is large enough for an aircraft to duct some of the engine exhaust out. By blowing out of the trailing edge, we reduce or even eliminate the base drag associated with the thick trailing edge.

Consider the velocity profile in Figure 10. In the non-distributed-propulsion case, the drag of the body is represented by the velocity deficit area created by the wake, namely, Area A. In the distributed-propulsion case, assuming the same sized wake (for the same body), the drag is now represented by the sum of Area B and C, which is smaller than Area A. The difference between Area A and the sum of Area B and C (which is equal to Area E) represents the base drag that is not present in the distributed-propulsion configuration.

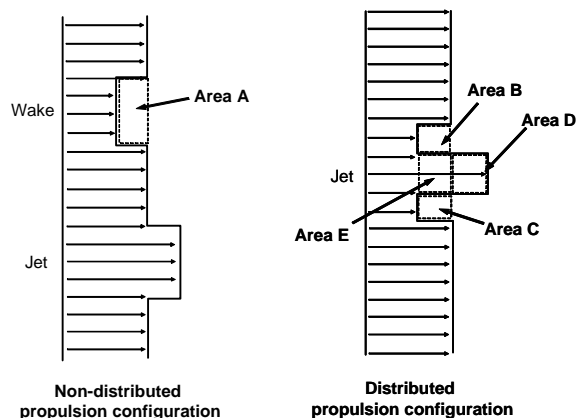


Figure 10: Illustration showing the difference between the velocity profile behind the body and jet for non-distributed-propulsion and distributed-propulsion configurations.

Another way of visualizing this effect is by considering the velocity profile relative to the body. In Figure 11, in relation to the body, the wake creates a ‘negative’ velocity component in the chordwise direction. Similarly, the jet produces a positive velocity component. The section of the wake behind the thick trailing edge is not present because it is being ‘filled’ in by the jet.

One important implication of this theory is that the propulsive efficiency is only dependent on the jet width and velocity of the propulsor. However, recall that the two are connected by the self-propelled condition.

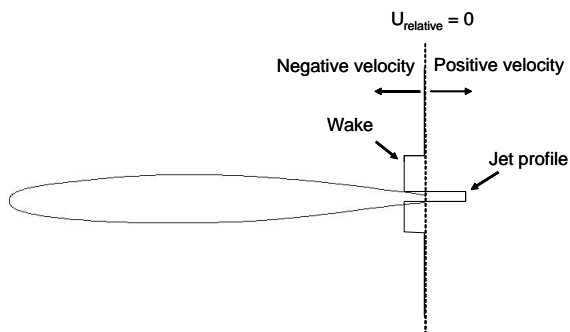


Figure 11: Figure shows relative velocity profile behind a streamlined body of a distributed-propulsion configuration, relative to the body.

Equation (3.5) shows that a smaller jet velocity relative to the freestream velocity results in a better propulsive efficiency. However, it is quite possible that a conventional propulsion arrangement could achieve a better propulsive efficiency by being able to generate the same amount of thrust at a smaller jet velocity. In a distributed-propulsion system, the jet velocity is limited by the available exit area of the trailing edge of the body. In a two-dimensional case, this is represented by the ‘height’ of the jet. A small jet height results in high jet velocities to produce the needed thrust. No such limit applies to the conventional arrangement, where the exit area out of the engine can be as large as needed to achieve a small jet velocity.

For a distributed-propulsion system to do better than the conventional arrangement, the trailing edge of the wing has to be thick enough to allow a low jet velocity. The logical question then should be: how thick should the trailing edge of an airfoil be for a distributed-propulsion system to achieve efficiencies better than conventional propulsion arrangements? To answer this, we considered a typical 10% t/c ratio supercritical airfoil which has a 0.5% chord thickness trailing edge. We found that to propel this airfoil at Mach 0.72 with a jet out of the trailing edge, a propulsive efficiency of 78% is achieved. Doubling the trailing edge thickness (1% chord length) will give a projected efficiency of 84%, but there may be adverse aerodynamic effects from increasing the trailing edge thickness.

The application of this theory is not solely limited to thick trailing edge wing sections. This theory can also be applied to wing sections with blowing out of the upper and lower wing surface close to the trailing edge, as shown in Figure 12. In this configuration, not only is the engine jet exhausted from the thick trailing edge, it is also exhausted from the surface of the wing through slots or holes. This allows for more exhaust area, allowing for a smaller jet velocity and hence a better propulsive efficiency for the same thrust.



Figure 12: Concept to which the distributed-propulsion theory can be applied. Blowing through the upper and lower surface of the wing through slots or holes allows for a larger area to exhaust, hence resulting in a lower velocity and better propulsive efficiency for the same thrust.

4. Application to a Blended-Wing-Body aircraft

To take advantage of the improvement in engine efficiency due to the close coupling between the aerodynamics and propulsion systems, Multi-Disciplinary Optimization (MDO) was used to design an aircraft tailored to use this distributed-propulsion concept. The Blended-Wing-Body aircraft configuration (shown in Figure 13) was chosen. The BWB configuration takes full advantage of the distributed-propulsion concept, being an ‘all-wing’ aircraft

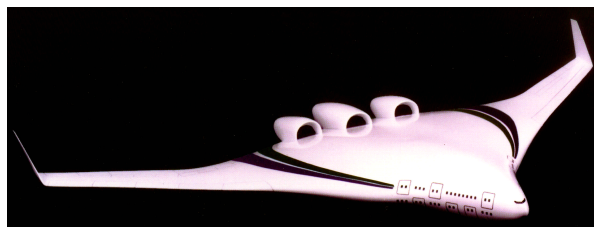


Figure 13: The Blended-Wing-Body aircraft with conventional propulsion.

The distributed-propulsion BWB aircraft will have a modest number of high bypass ratio engines (about eight) buried inside the structure, distributed across the span. Part of the engine cold air exhaust will be ducted to exit out the trailing edge of the wing. The rest of the engine exhaust (the rest of the cold air exhaust and the hot core exhaust) will be ejected through a conventional nozzle.

The BWB aircraft is described using 21 design variables, including geometric quantities such as the chord length, thickness to chord ratio (t/c) at five semi-span stations, the position of the semi-span stations (h), the quarter chord sweep of the wing and non-geometric design variables that include the average cruise altitude, fuel weight and engine thrust.

The distributed-propulsion BWB aircraft was optimized to minimize the takeoff gross weight, subject to 19 inequality constraints. These include field performance, fuel volume, range and stability & control constraints. Passenger cabin area and cabin egress

constraints were also implemented. Reference [7] describes the MDO problem statement in detail.

Low and medium fidelity analytical models were used to estimate the aerodynamic, propulsion, structures and flight performance of the BWB aircraft. The entire MDO framework was validated by comparing published BWB design results [9], [10] with those obtained from the distributed-propulsion BWB MDO code.

In addition to modeling the effect of distributed-propulsion on the propulsive efficiency described in this paper, other distributed-propulsion models were also included. These included the effect of losses in thrust due to ducting part of the engine exhaust, the effect on the induced drag of the aircraft, and the additional weight due to the exhaust ducting systems.

Two different BWB aircraft were optimized: a conventional BWB and a distributed-propulsion BWB configuration. Both aircraft are designed for a 7000 nmi mission range with a 500 nmi reserve range, cruising at a Mach number of 0.85. The passenger capacity is 800 passengers in a three-class configuration. The field performance requires a maximum 11,000 ft takeoff and landing field length.

Detailed results for the MDO design can be found in Reference [7]. The distributed-propulsion BWB design is 4.45% lighter than the conventional BWB aircraft. It also requires 2.3% less fuel to perform the same mission. Both designs have the same aspect ratio of about 5.6, and cruise at nearly the same lift coefficient. In general, the optimum distributed-propulsion BWB design has a higher quarter chord sweep and the average cruise altitude is about 2000 ft lower than its comparator. The distributed-propulsion BWB design differs from the conventional BWB design in that the chord lengths of the first three sections are smaller. In turn, the t/c ratios at these sections are higher to meet the passenger cabin thickness constraints. This results in the distributed-propulsion BWB aircraft having a 4% higher wing loading (W/S). The distributed-propulsion BWB aircraft also requires 15% less total thrust, which corresponds to a T/W decrease of 11%.

The results quoted reflect the cumulative effect of all the distributed-propulsion effects applied to the BWB aircraft. When optimizations were performed starting from the conventional BWB design and individually implementing the distributed-propulsion effects, the effect of the savings in propulsive efficiency could be quantified. It was found that the savings due to the increased propulsive efficiency decreased the aircraft TOGW by 1.46%. This led to a reduction in fuel weight of 2.7%. There was also a reduction in wing weight of 3.0%, as a consequence of an almost 2% smaller wing planform area.

5. Conclusions

A new model for distributed-propulsion applied to aircraft has been developed and then incorporated into an MDO design formulation. One effect of distributed-propulsion is its impact on the propulsive efficiency. It has been theorized that there will be an increase in propulsive efficiency when the engine jet is exhausted out the trailing edge of an aircraft wing. Until now, no mathematical assessment has been done to understand the mechanism or to provide quantitative predictions of the change in efficiency. Starting from first principles, a mathematical description of this effect was formulated. By considering simple, idealized, representative cases, and comparing them to a conventional propulsion arrangement, a quantitative assessment of the increase in propulsive efficiency was made. The jet 'fills in' the wake behind the body, resulting in a better overall aerodynamic/propulsion system.

To quantify the effects of this increase in efficiency, the limiting cases with maximum and minimum benefits of this effect were considered. In the formulation, we assume a minimum propulsive efficiency of 80%, which corresponds to a conventional arrangement where a modern turbofan engine is installed on pylons. The ratio of the thrust from the wing trailing edge jets to the total thrust is determined by setting it equal to the ratio of the friction and wave drag to the total drag. This results in a maximum attainable propulsive efficiency of 88% - 90%. By identifying the bounds in attainable propulsive efficiency using a distributed-propulsion system, we get a formulation by which the projected propulsive efficiency of a distributed-propulsion system can be determined.

Together with other distributed-propulsion models, this formulation was implemented in an MDO framework to design a distributed-propulsion BWB aircraft. This and a conventional BWB aircraft are designed to carry 800 passengers at a range of 7000 nmi, cruising at a Mach number of 0.85. The distributed-propulsion BWB aircraft was found to be 4.4% lighter than the conventional BWB comparator aircraft design, using 2.3% less fuel to perform the same mission. The effect of the savings in propulsive efficiency alone decreases the aircraft TOGW by 1.46% and reduces the fuel weight by 2.7%.

6. Acknowledgements

The Systems Analysis Branch at NASA Langley supported our work. We would like to acknowledge their help with information, insight and material. We would like to specifically acknowledge William M. Kimmel and Mark Guynn at NASA Langley for their support and help in this work.

7. References

- [1] Attinello, J. S., "The Jet Wing," IAS Preprint No. 703, IAS 25th Annual meeting, Jan. 28-31, 1957.
- [2] Kuchemann, D., *The Aerodynamic Design of Aircraft*, Pergamon Press, New York, 1978, pp. 229.
- [3] *NASA Aeronautics Blueprint: Toward a Bold New Era in Aviation*, NASA,
http://www.aerospace.nasa.gov/aero_blueprint/cover.html
- [4] *Marine Engineering*, Vol. 1, Society of Naval Architect & Marine Engineers, Ed. Herbert Lee Seward, pp. 10-11.
- [5] Hill, P. and Peterson, C., *Mechanics and Thermodynamics of Propulsion*, 2nd Ed., Addison-Wesley, New York, 1992.
- [6] Stinton, D., *The Anatomy of the Airplane*, 2nd Ed., American Institute of Aeronautics and Astronautics, Reston, VA., 1998, pp153.
- [7] Ko, Y.-Y. A, "The Multidisciplinary Design Optimization of a Distributed Propulsion Blended-Wing-Body Aircraft," Ph.D. Dissertation, Virginia Polytechnic Institute & State University, April, 2003.
- [8] Harris, C. D., "NASA Supercritical Airfoils: A Matrix of Family Related Airfoils," NASA TP 2969, March 1990.
- [9] Liebeck, R. H., Page, M. A., Rawdon, B. K., Scott, P. W., and Wright, R. A., "Concepts for Advanced Subsonic Transports" NASA CR 4624, Sept. 1994.
- [10] Liebeck, R. H., Page, M. A., Rawdon, B. K., Girvin, R. R., Scott, P. W., Potsdam, M. A., Bird, R. S., Wakayama, S., Hawley, A. V., Rowland, G. T., "Blended-Wing-Body Configuration Control Document (1-26-96) CCD-2," McDonnell Douglas Aerospace, Long Beach, CA, Jan., 1996.